GEOLOGY | THE GEOLOGICAL SOCIETY OF AMERICA®

https://doi.org/10.1130/G48333.1

Manuscript received 27 August 2020
Revised manuscript received 26 November 2020
Manuscript accepted 3 December 2020

Published online 5 February 2021

Metal-induced stress in survivor plants following the end-Permian collapse of land ecosystems

Daoliang Chu[1]*, Jacopo Dal Corso[1], Wenchao Shu[1], Haijun Song[1], Paul B. Wignall[2], Stephen E. Grasby[3], Bas van de Schootbrugge[4], Keqing Zong[5], Yuyang Wu[1] and Jinnan Tong[1]

[1]State Key Laboratory of Biogeology and Environmental Geology, School of Earth Sciences, China University of Geosciences, Wuhan 430074, China

[2]School of Earth and Environment, University of Leeds, Leeds LS2 9JT, UK

[3]Geological Survey of Canada, Natural Resources Canada, Calgary, Alberta T2L2A7, Canada

[4]Department of Earth Sciences, Utrecht University, Utrecht 3584 CB, Netherlands

[5]School of Earth Sciences, State Key Laboratory of Geological Processes and Mineral Resources, China University of Geosciences, Wuhan 430074, China

ABSTRACT

Teratological spores and pollen are widespread in sediments that record the Permian-Triassic mass extinction. The malformations are thought to be the result of extreme environmental conditions at that time, but the mutagenic agents and the precise timing of the events remain unclear. We examined the abundance of teratological sporomorphs and metal concentrations in a Permian-Triassic tropical peatland succession of southwestern China. We find a significant peak of spore tetrads of lycopsid plants (as much as 19% of all sporomorphs) coeval with increases in Cu and Hg concentrations above the main terrestrial extinction interval, which marks the loss of Permian *Gigantopteris* forests, increased wildfire activity, and the disappearance of coal beds. Thus, in tropical peatlands, mutagenesis affected only surviving plants. Mutagenesis was likely caused by metal toxicity, linked to increased Hg and Cu loading, but was not itself a direct cause of the terrestrial crisis.

INTRODUCTION

The Permian-Triassic mass extinction (PTME) had a catastrophic impact on both marine and terrestrial ecosystems and was the most severe crisis of the Phanerozoic (e.g., Wignall, 2015). The contemporaneous eruption of the Siberian Traps large igneous province is thought to have been the main trigger of the biological crisis, with the release of vast quantities of volatiles such as CO_2, SO_2, organohalogens, and metals to the atmosphere resulting in the collapse of the biosphere (Beerling et al., 2007; Bond and Wignall, 2014; Burgess et al., 2017; Broadley et al., 2018). Work in Australia and southwestern China showed that collapse of the terrestrial ecosystems occurred prior to the marine mass extinction (Fielding et al., 2019; Chu et al., 2020). The loss of terrestrial ecosystems is evidenced by the sudden disappearance of the *Gigantopteris* flora and coal swamps, an abrupt drop to very low total organic carbon (TOC) content of coastal sediments, and frequent wildfires in terrestrial sections of southwestern China (Chu et al., 2020; Dal Corso et al., 2020). Some vegetation survived the collapse of the Permian terrestrial ecosystems in the tropics, as seen in southwestern China, where the luxuriant Permian *Gigantopteris*-dominated rainforests were replaced by herblands comprising almost monospecific lycophyte populations (Feng et al., 2020).

Spore tetrads and pollen malformations have been observed globally in sediments deposited during the PTME and are commonly reported in relatively high abundances in some quantitative studies (e.g., Looy et al., 2001, 2005; Visscher et al., 2004; Hochuli et al., 2017; Fig. 1). These malformations have been attributed to the effects on plants of extreme environmental conditions (Visscher et al., 2004; Foster and Afonin, 2005; Hochuli et al., 2017; Benca et al., 2018). However, no consensus exists on the actual stressor. Increased levels of ultraviolet-B (UV-B) radiation associated with ozone-layer depletion has been invoked as a possible mutating agent (e.g., Visscher et al., 2004), but no independent evidence has yet been found. Pollution of the atmosphere by volcanic volatiles, in particular Hg, has been postulated as a possible cause of malformed plant spores (Hochuli et al., 2017). Similarly, Lindström et al. (2019) suggested that a correlation between teratological sporomorphs and Hg enrichments across the end-Triassic mass extinction indicates mutagenic effects of emissions from the Central Atlantic magmatic province. Phytotoxic volcanic gas emissions can cause abnormalities in plants and their spores or pollen, including stunted growth, lesions, malformed spores and pollen, and tetrads (e.g., Lindström et al., 2019).

A marked increase of Hg concentrations, as well as of other heavy metals like Cu, has been found in many Permian-Triassic boundary marine and terrestrial successions (Grasby et al., 2015, 2019; Shen et al., 2019; Wang et al., 2019; Chu et al., 2020). Improved chronology of the terrestrial records of the PTME (e.g., Chu et al., 2020), where floral changes are better documented, allows exploration of the cause-and-effect relationship between the collapse of ecosystems on land, the geochemical changes observed, and the occurrence of mutated spores and pollen. Hence, we investigated phytotoxic heavy metal concentrations and stress responses of terrestrial plants, specifically in the record of spore tetrad abundances, in a well-calibrated terrestrial Permian-Triassic boundary section in southwestern China.

MATERIALS AND METHODS

We studied the ZK4703 borehole from the South China block (drilled 15 km south

*E-mail: chudl@cug.edu.cn

CITATION: Chu, D., et al., 2021, Metal-induced stress in survivor plants following the end-Permian collapse of land ecosystems: Geology, v. 49, p. 657–661, https://doi.org/10.1130/G48333.1

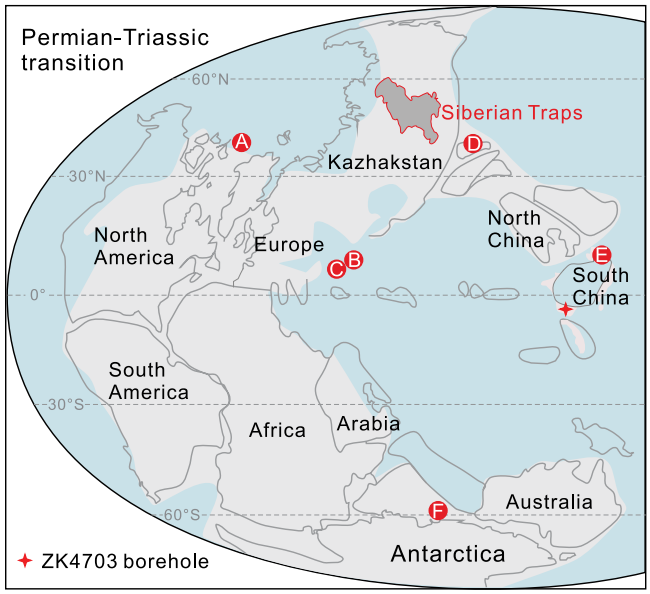

Figure 1. Paleogeographic map showing locations of lycopsid spore tetrad and metal enrichment occurrences at the Permian-Triassic transition, and location of the ZK4703 borehole (25.54151°N, 104.28994°E, present-day coordinates). (A) Sverdrup Basin, Arctic Canada. (B) Hungary. (C) Italy. (D) Dalongkou, Junggar Basin, northwestern China. (E) Meishan, South China. (F) India. Distribution data for lycopsid tetrads are from Visscher et al. (2004, and references therein) and Looy et al. (2005 and references therein). Data for metal elements, including Hg, Cu, Ni, Pb, and Zn, are from Sanei et al. (2012), Grasby et al. (2015), Rampino et al. (2017), Shen et al. (2019), and Sial et al. (2020). Base map is after Muttoni et al. (2009).

of Fuyuan at the Dahe Mine [25.54151°N, 104.28994°E]). It records paralic conditions at equatorial paleolatitudes during the Permian-Triassic transition (Fig. 1). The borehole encompasses, in ascending order, the Changhsingian upper Xuanwei, Permian-Triassic transitional Kayitou, and earliest Triassic Dongchuan Formations (Fig. 2). Mudrock samples were processed using standard palynological acid maceration techniques involving digestion of 40 g of mudstone in hydrochloric and hydrofluoric acid, then dilution with ultrapure water to reach neutral pH. The residue was sieved over a 100 μm mesh screen, and both size fractions were collected. The organic and inorganic residues in the <100 μm size fractions were separated using $ZnCl_2$. Ten dry slides were sealed by neutral gum for each sample. To assess the percentage of the lycopsid spore tetrads (herein referred to as tetrads), all normal and tetrad specimens of spores were counted separately within the dry slides from each sample using a Zeiss Axio Scope A1 microscope until ≥100 specimens were counted or ten entire slides were scanned. Cu and Al contents in shales and mudstones were measured using an Agilent 7700e inductively coupled plasma–mass spectrometer at Wuhan Sample-Solution Analytical Technology Co., Ltd. (Wuhan, China). Data for organic $\delta^{13}C$ ($\delta^{13}C_{org}$), TOC content, and Hg concentrations are from our previous work (Chu et al., 2020).

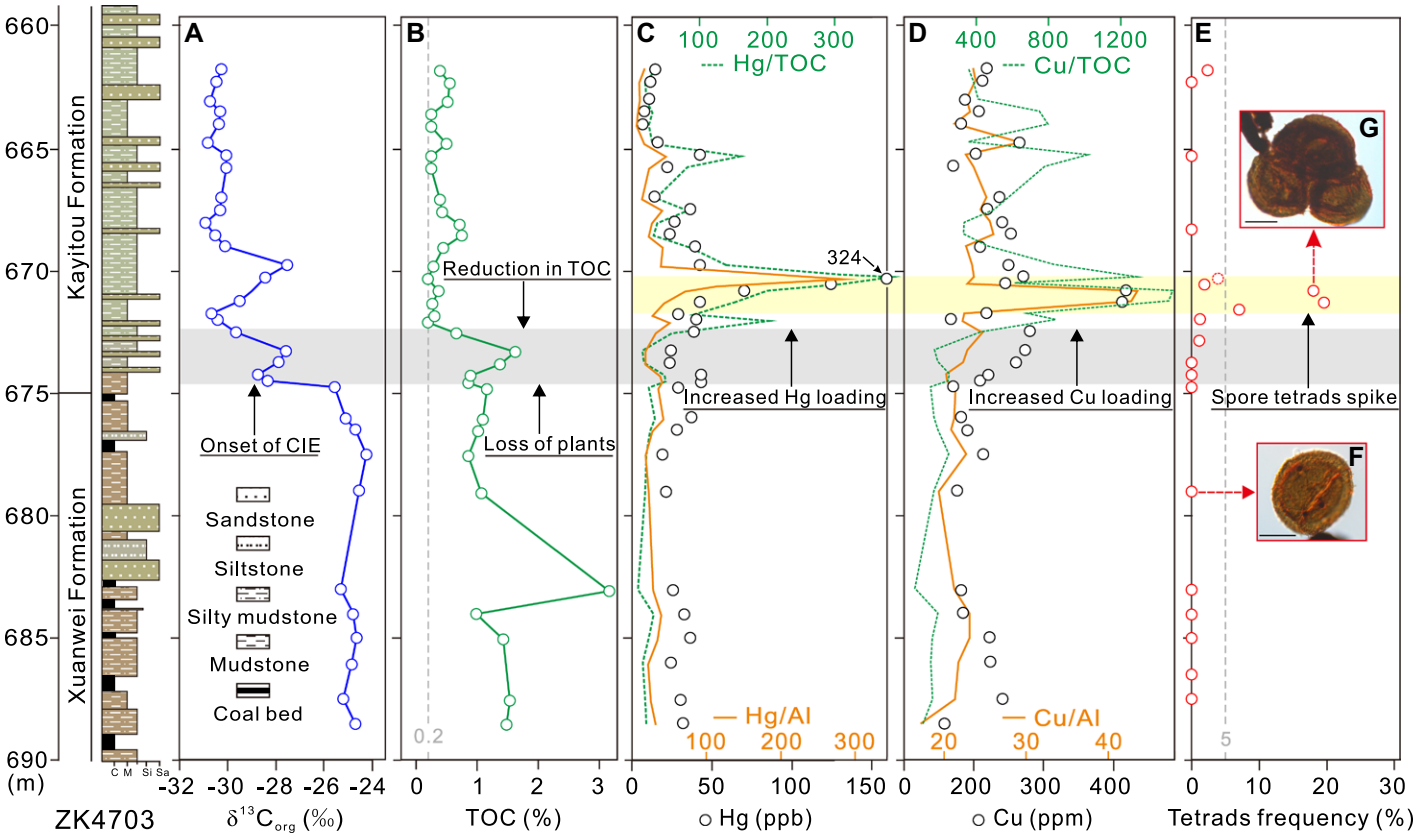

Figure 2. Lithological column and organic carbon isotopes ($\delta^{13}C_{org}$) (A), total organic carbon (TOC) (B), Hg concentration and Hg/Al and Hg/TOC ratios (C), Cu concentration and Cu/Al and Cu/TOC ratios (D), and tetrad frequency as proportion of total spores (E) for ZK4703 borehole, southwestern China (25.54151°N, 104.28994°E), and photographs of normal (F) and tetrad (G) *Aratrisporites* (scale bar is 20 μm). Log shows lithologies (C—coal; M—mudrocks; Si—siltstone; Sa—sandstone) with approximate representation of color. Gray bar shows onset of negative carbon isotope excursion (CIE) coupled with loss of *Gigantopteris* flora. Yellow bar shows enrichment in heavy metals and tetrad spike. Data for organic carbon isotopes, TOC, Hg concentration, and Hg/TOC ratios are from Chu et al. (2020).

RESULTS

The palynological and geochemical data are provided in the Supplemental Material[1] and in Figure 2. Cu concentrations are plotted along with values normalized to Al, to account for potential lithologic changes, and to TOC, given that Cu bonds with organic matter in terrestrial plants and soil. Cu values are relatively constant from the Xuanwei Formation to the base of the Kayitou Formation but increase in concentration (and also Cu/Al and Cu/TOC) above this, reaching a peak Cu value of 417 ppm (Fig. 2D). Hg and Hg/TOC rise above background levels following the drop in TOC and immediately above the onset of a negative carbon isotope excursion (CIE) (Fig. 2; Chu et al., 2020). High Hg concentrations are observed in a ~2 m interval of the lower part of Kayitou Formation where Hg increased >10× above background levels (as high as 324 ppb) (Fig. 2C). Other heavy minerals, e.g., Ni, Pb, Cr, and Zn, show very low concentrations and no changes across the section (see Table S1 in the Supplemental Material).

Temporal trends of tetrad abundances for the ZK4703 core were examined by calculating their frequency in the total number of spores. Spore tetrads are rare and their frequency never exceed 1% of all spores from the Xuanwei Formation to the base of the Kayitou Formation (Fig. 2E). A distinct peak of tetrads is then observed in the Kayitou Formation where Hg and Cu enrichments occur. At this level, as much as 19% of all spores are tetrads (Fig. 2E). The peak in tetrad abundance is precisely synchronous with the Cu peak (Figs. 2D and 2E). All the tetrads and normal spores showed the same taphonomic features and thermal alteration stage throughout the succession, indicated by the uniform phytoclast composition and palynomorph color (Fig. 3; Fig. S1; Chu et al., 2020), ruling out selective recycling. Tetrads are essentially absent below and above their interval of peak abundance. The lycopsid tetrads belong to *Aratrisporites yunnanensis* and *Lapposisporites echinatus* (e.g., Ouyang and Norris, 1999).

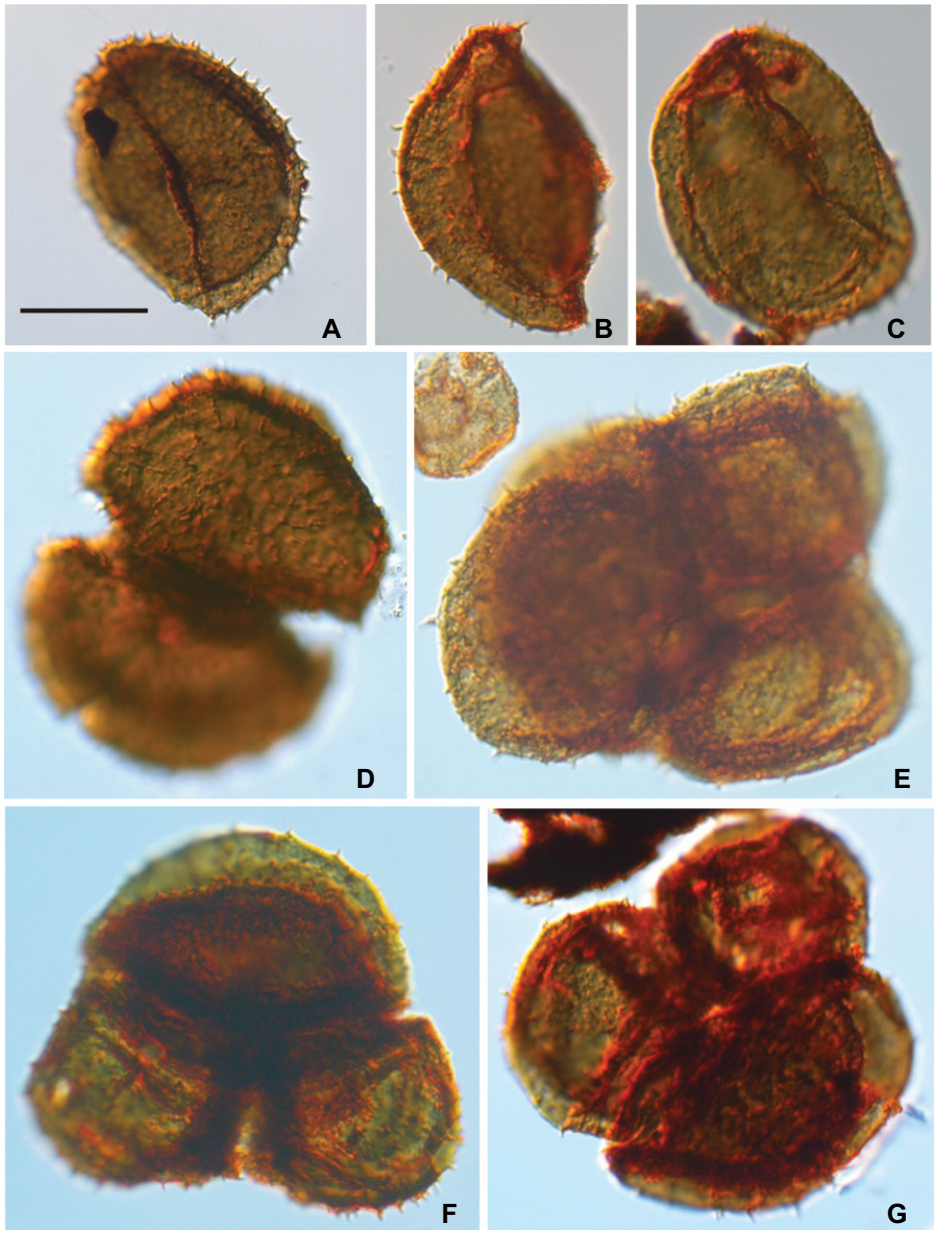

Figure 3. Selection of normal and tetrad spores from sample ZK-41 of ZK4703 borehole, southwestern China (25.54151°N, 104.28994°E). (A–C) *Aratrisporites* spp. (normal). (D) *Lapposisporites echinatus* (dyad or one half of tetrad). (E–G) Unseparated tetrads of *Lapposisporites echinatus*. Scale bar is 20 µm.

DISCUSSION

In southwestern China, an increase in lycopsid tetrads occurred after the collapse of the terrestrial ecosystem, which is marked by a sharp decline in TOC to almost 0%; it coincides with an interval of increased Cu and Hg concentrations and occurs within the negative CIE (Fig. 2). Correlation of the $\delta^{13}C_{org}$ and Hg records indicates that the tetrad spike is synchronous with the marine mass extinction (Chu et al., 2020).

In both extant and fossil assemblages, malformed sporomorphs >5% of the total population indicates environmental stress (e.g., Lindström et al., 1997; Foster and Afonin, 2005), and modern studies show that an increased abundance of teratologic sporomorphs is an indicator of local environmental disturbance (e.g., Mičieta and Murín, 1996). The peak frequencies of tetrads in our study (6%–19%) therefore indicate considerable environmental stress. However, the increase in lycopsid tetrads occurs immediately after the floral extinctions and last coal beds, indicating ecological pressure was focused on the surviving lycopsids. Intriguingly, lycopsids do not display this stress indicator at the time of extinction amongst the Permian flora. Similar increases in immature tetrads of survivor lycophytes have been found in Greenland and Norway and have been explained as the possible effect of prolonged UV-B radiation on plants or atmospheric pollution by toxic metals (Visscher et al., 2004; Hochuli et al., 2017). Lycopsids were widespread during the PTME interval and are considered stress-tolerant opportunistic plants, capable of surviving the terrestrial catastrophe (e.g., Looy et al., 2001; Visscher et al., 2004). However, even these hardy plants were clearly suffering high levels of stress in the extinction aftermath.

Data normalized for TOC and Al contents show that the Hg and Cu peaks are not due to changes in organic carbon contents nor lithology

[1]Supplemental Material. Description of the studied borehole, analytical methods, supplemental figure, and data tables. Please visit https://doi.org/10.1130/GEOL.S.13584935 to access the supplemental material, and contact editing@geosociety.org with any questions.

but are instead the result of enhanced metal loading. To date, a sharp Hg spike has been widely observed in numerous marine PTME intervals (e.g., Grasby et al., 2015, 2019; Wang et al., 2019) as well as in some terrestrial records (Shen et al., 2019; Chu et al., 2020). The sources of Hg at the Permian-Triassic transition are multiple (e.g., Grasby et al., 2019, 2020; Dal Corso et al., 2020, and references therein). Modeling suggests oxidation of terrestrial biomass, and increased soil erosion related to the collapse of the terrestrial ecosystems, can explain the sharp spike in Hg, which is observed in both terrestrial and marine depositional environments, and the coeval negative Δ^{199}Hg and δ^{13}C values recorded at the marine PTME stratigraphic level, while volcanism could account for a longer-term increase in Hg loading (Grasby, et al., 2020; Dal Corso et al., 2020). The release of thermogenic Hg produced from organic-rich sediments in contact with Siberian Traps intrusions could have been an additional source of Hg (Sanei et al., 2012). Cu could also have derived from multiple sources, although fewer data are available to fully understand its behavior at the Permian-Triassic boundary. Cu spikes have been observed in Spitsbergen (Norway) and have been explained as related to higher loading rates from the volcanic ash of Siberian Traps eruptions (Grasby et al., 2015). Cu is also present in high amounts in soil, and a large part of it (~36%) is bound to organic matter (e.g., Adriano, 1986); Cu is an essential element during photosynthesis by higher plants (Nagajyoti et al., 2010). Therefore, a mechanism of Cu release from organic-matter oxidation and soil erosion, similar to that proposed for Hg (Dal Corso et al., 2020), can be also hypothesized.

The coincidence between metal enrichment and relatively abundant spore tetrads that we observe (Fig. 2) suggests that Hg and Cu may have acted as phytotoxic pollutants and represented a stressor on terrestrial ecosystems after the terrestrial mass extinction. Metal toxicity is known to induce oxidative stress by triggering the generation of reactive oxygen species (ROSs), which is linked to oxidation of proteins and membrane lipids and to alterations of DNA (e.g., Nagajyoti et al., 2010; Lindström et al., 2019). ROSs can damage the DNA strand or interact with proteins used to repair the DNA, eventually causing mutagenesis; damaged DNA can then be transferred to the next generation (e.g., Kültz, 2005). Hg is well known as one of the most toxic metals and could have caused inhibition of plant growth and photosynthesis, oxidative stress, and damage of proteins and DNA (Azevedo et al., 2018). Cu is a very important micronutrient and essential component of proteins for plants; however, excess Cu also plays a cytotoxic role (Angelé-Martínez et al., 2017; Nagajyoti et al., 2010). Just like Hg-induced genotoxicity, Cu toxicity can also generate oxidative stress with ROSs, inducing growth inhibition and lipid peroxidation (İşeri et al., 2011). We therefore propose that metal genotoxicity most likely caused the observed malformations in the survivor lycophytes at the PTME, as also invoked for the marine extinction (Grasby et al., 2015, 2020), but was not observed during the terrestrial extinction. Ozone depletion during the PTME is unproven; its evaluation awaits the development of an independent test for ancient ozone levels. However, given the global distribution of mutated sporomorphs, UV-B radiation as a mutagenic mechanism remains contentious because ozone can be rapidly replenished in the atmosphere, making global ozone destruction difficult (Black et al., 2014).

In summary, the terrestrial successions of southwestern China offer a detailed picture of terrestrial events: vegetation first entered into crisis, Permian flora declined, and wildfire activity increased (Chu et al., 2020); then, the terrestrial ecosystems suddenly collapsed (at the level of the onset of the marine PTME), as evidenced by the disappearance of the *Gigantopteris* forests and coal deposits, causing sediment TOC to fall to ~0%. This was immediately followed by increased Hg and Cu loading, causing a major increase in the abundance of undeveloped spore tetrads (Fig. 2). The reason for the extinction of *Gigantopteris* flora remains unknown because sporomorphs' mutagenesis, in southwestern China, was only observed in the survivor lycophytes, and no or <1% unseparated spore tetrads are found before this interval, when the decline of the Permian forests and increased wildfire activity are recorded (Fig. 2).

CONCLUSIONS

The record of spore tetrad abundances and metal concentrations during the Permian-Triassic mass extinction in a well-preserved core (ZK4703) encompassing the terrestrial record of southwestern China provides insight into the terrestrial ecosystem collapse. A significant peak of lycophyte tetrads occurs in the immediate aftermath of a sharp TOC drop, which is associated with the loss of the Permian *Gigantopteris* flora and coal swamps. Both Hg and Cu concentrations show a large peak during the tetrad acme. The close temporal relationship between extinction, metal concentrations, and spore teratology suggests that survivor lycophyte plants were under huge stress after the loss of the Permian *Gigantopteris* forests. The mutagenesis of the reproductive organs was likely driven by environmental pollution linked to a sudden rise of Hg and Cu loading into the system that followed. Importantly, this toxic stress postdates the terrestrial extinction and indicates some other, as yet undiagnosed, mechanism caused the losses.

ACKNOWLEDGMENTS

We are grateful to reviewers D. Bond, S. Lindström, and C. Fielding for their constructive comments. This study was supported by the National Natural Science Foundation of China (grants 42072025 and 41821001), and the UK Natural Environment Research Council's Eco-PT project (grant NE/P01377224/1), which is a part of the Biosphere Evolution, Transitions and Resilience (BETR) Program.

REFERENCES CITED

Adriano, D.C., 1986, Trace Elements in the Terrestrial Environment: Berlin, Heidelberg, Springer Press, 533 p., https://doi.org/10.1007/978-1-4757-1907-9.

Angelé-Martínez, C., Nguyen, K.V.T., Ameer, F.S., Anker, J.N., and Brumaghim, J.L., 2017, Reactive oxygen species generation by copper(II) oxide nanoparticles determined by DNA damage assays and EPR spectroscopy: Nanotoxicology, v. 11, p. 278–288, https://doi.org/10.1080/17435390.2017.1293750.

Azevedo, R., Rodriguez, E., Mendes, R.J., Mariz-Ponte, N., Sario, S., Lopes, J.C., Ferreira de Oliveiraet, J.M.P., and Santos, C., 2018, Inorganic Hg toxicity in plants: A comparison of different genotoxic parameters: Plant Physiology and Biochemistry, v. 125, p. 247–254, https://doi.org/10.1016/j.plaphy.2018.02.015.

Beerling, D.J., Harfoot, M., Lomax, B., and Pyle, J.A., 2007, The stability of the stratospheric ozone layer during the end-Permian eruption of the Siberian Traps: Philosophical Transactions of the Royal Society of London A, v. 365, p. 1843–1866, https://doi.org/10.1098/rsta.2007.2046.

Benca, J.P., Duijnstee, I.A.P., and Looy, C.V., 2018, UV-B–induced forest sterility: Implications of ozone shield failure in Earth's largest extinction: Science Advances, v. 4, e1700618, https://doi.org/10.1126/sciadv.1700618.

Black, B.A., Lamarque, J.F., Shields, C.A., Elkins-Tanton, L.T., and Kiehl, J.T., 2014, Acid rain and ozone depletion from pulsed Siberian Traps magmatism: Geology, v. 42, p. 67–70, https://doi.org/10.1130/G34875.1.

Bond, D.P.G., and Wignall, P.B., 2014, Large igneous provinces and mass extinctions: An update, *in* Keller, G., and Kerr, A.C., eds., Volcanism, Impacts, and Mass Extinctions: Causes and Effects: Geological Society of America Special Paper 505, p. 29–55, https://doi.org/10.1130/2014.2505(02).

Broadley, M.W., Barry, P.H., Ballentine, C.J., Taylor, L.A., and Burgess, R., 2018, End-Permian extinction amplified by plume-induced release of recycled lithospheric volatiles: Nature Geoscience, v. 11, p. 682–687, https://doi.org/10.1038/s41561-018-0215-4.

Burgess, S.D., Muirhead, J.D., and Bowring, S.A., 2017, Initial pulse of Siberian Traps sills as the trigger of the end-Permian mass extinction: Nature Communications, v. 8, 164, https://doi.org/10.1038/s41467-017-00083-9.

Chu, D.L., et al., 2020, Ecological disturbance in tropical peatlands prior to marine Permian-Triassic mass extinction: Geology, v. 48, p. 288–292, https://doi.org/10.1130/G46631.1.

Dal Corso, J., Mills, B.J.W., Chu, D.L., Newton, R.J., Mather, T.A., Shu, W.C., Wu, Y.Y., Tong, J.N., and Wignall, P.W., 2020, Permo-Triassic boundary carbon and mercury cycling linked to terrestrial ecosystem collapse: Nature Communications, v. 11, 2962, https://doi.org/10.1038/s41467-020-16725-4.

Feng, Z., Wei, H.B., Guo, Y., He, X.Y., Sui, Q., Zhou, Y., Liu, H.Y., Gou, X.D., and Lu, Y., 2020, From rainforest to herbland: New insights into land plant responses to the end-Permian mass extinction: Earth-Science Reviews, v. 204, 103153, https://doi.org/10.1016/j.earscirev.2020.103153.

Fielding, C.R., et al., 2019, Age and pattern of the southern high-latitude continental end-Permian

extinction constrained by multiproxy analysis: Nature Communications, v. 10, 385, https://doi.org/10.1038/s41467-018-07934-z.
Foster, C.B., and Afonin, S.A., 2005, Abnormal pollen grains: An outcome of deteriorating atmospheric conditions around the Permian-Triassic boundary: Journal of the Geological Society, v. 162, p. 653–659, https://doi.org/10.1144/0016-764904-047.
Grasby, S.E., Beauchamp, B., Bond, D.P.G., Wignall, P., Talavera, C., Galloway, J.M., Piepjohn, K., Reinhardt, L., and Blomeier, D., 2015, Progressive environmental deterioration in northwestern Pangea leading to the latest Permian extinction: Geological Society of America Bulletin, v. 127, p. 1331–1347, https://doi.org/10.1130/B31197.1.
Grasby, S.E., Them, T.R., II, Chen, Z.H., Yin, R.S., and Ardakani, O.H., 2019, Mercury as a proxy for volcanic emissions in the geologic record: Earth-Science Reviews, v. 196, 102880, https://doi.org/10.1016/j.earscirev.2019.102880.
Grasby, S.E., Liu, X.J., Yin, R.S., Ernst, R.E., and Chen, Z.H., 2020, Toxic mercury pulses into late Permian terrestrial and marine environments: Geology, v. 48, p. 830–833, https://doi.org/10.1130/G47295.1.
Hochuli, P.A., Schneebeli-Hermann, E., Mangerud, G., and Bucher, H., 2017, Evidence for atmospheric pollution across the Permian-Triassic transition: Geology, v. 45, p. 1123–1126, https://doi.org/10.1130/G39496.1.
İşeri, Ö.D., Körpe, D.A., Yurtcu, E., Sahin, F.I., and Haberal, M., 2011, Copper-induced oxidative damage, antioxidant response and genotoxicity in *Lycopersicum esculentum* Mill. and *Cucumis sativus* L.: Plant Cell Reports, v. 30, 1713, https://doi.org/10.1007/s00299-011-1079-x.
Kültz, D., 2005, Molecular and evolutionary basis of the cellular stress response: Annual Review of Physiology, v. 67, p. 225–257, https://doi.org/10.1146/annurev.physiol.67.040403.103635.
Lindström, S., McLoughlin, S., and Drinnan, A.N., 1997, Intraspecific variation of taeniate bisaccate pollen within Permian glossopterid sporangia, from the Prince Charles Mountains, Antarctica: International Journal of Plant Sciences, v. 158, p. 673–684, https://doi.org/10.1086/297479.
Lindström, S., Sanei, H., van de Schootbrugge, B., Pedersen, G.K., Lesher, C.E., Tegner, C., Heunisch, C., Dybkjær, K., and Outridge, P.M., 2019, Volcanic mercury and mutagenesis in land plants during the end-Triassic mass extinction: Science Advances, v. 5, eaaw4018, https://doi.org/10.1126/sciadv.aaw4018.
Looy, C.V., Twitchett, R.J., Dilcher, D.L., Van Konijnenburg-Van Cittert, J.H.A., and Visscher, H., 2001, Life in the end-Permian dead zone: Proceedings of the National Academy of Sciences of the United States of America, v. 98, p. 7879–7883 https://doi.org/10.1073/pnas.131218098.
Looy, C.V., Collinson, M.E., Van Konijnenburg-Van Cittert, J.H.A., Visscher, H., and Brain, A.P., 2005, The ultrastructure and botanical affinity of end-Permian spore tetrads: International Journal of Plant Sciences, v. 166, p. 875–887 https://doi.org/10.1086/431802.
Mičieta, K., and Murín, G., 1996, Microspore analysis for genotoxicity of a polluted environment: Environmental and Experimental Botany, v. 36, p. 21–27, https://doi.org/10.1016/0098-8472(95)00050-X.
Muttoni, G., Gaetani, M., Kent, D.V., Sciunnach, D., Angiolini, L., Berra, F., Garzanti, E., Mattei, M., and Zanchi, A., 2009, Opening of the Neo-Tethys Ocean and the Pangea B to Pangea A transformation during the Permian: GeoArabia, v. 14, p. 17–48.
Nagajyoti, P.C., Lee, K.D., and Sreekanth, T.V.M., 2010, Heavy metals, occurrence and toxicity for plants: A review: Environmental Chemistry Letters, v. 8, p. 199–216, https://doi.org/10.1007/s10311-010-0297-8.
Ouyang, S., and Norris, G., 1999, Earliest Triassic (Induan) spores and pollen from the Junggar Basin, Xinjiang, northwestern China: Review of Palaeobotany and Palynology, v. 106, p. 1–56, https://doi.org/10.1016/S0034-6667(98)00078-5.
Rampino, M.R., Rodriguez, S., Baransky, E., and Cai, Y., 2017, Global nickel anomaly links Siberian Traps eruptions and the latest Permian mass extinction: Scientific Reports, v. 7, e12416, https://doi.org/10.1038/s41598-017-12759-9.
Sanei, H., Grasby, S.E., and Beauchamp, B., 2012, Latest Permian mercury anomalies: Geology, v. 40, p. 63–66, https://doi.org/10.1130/G32596.1.
Shen, J., Yu, J.X., Chen, J.B., Algeo, T.J., Xu, G.Z., Feng, Q.L., Shi, X., Planavsky, N.J., Shu, W.C., and Xie, S.C., 2019, Mercury evidence of intense volcanic effects on land during the Permian-Triassic transition: Geology, v. 47, p. 1117–1121, https://doi.org/10.1130/G46679.1.
Sial, A.N., et al., 2020, Globally enhanced Hg deposition and Hg isotopes in sections straddling the Permian-Triassic boundary: Link to volcanism: Palaeogeography, Palaeoclimatology, Palaeoecology, v. 540, 109537, https://doi.org/10.1016/j.palaeo.2019.109537.
Visscher, H., Looy, C.V., Collinson, M.E., Brinkhuis, H., van Konijnenburg-van Cittert, J.H.A., Kürschner, W.M., and Sephton, M.A., 2004, Environmental mutagenesis during the end-Permian ecological crisis: Proceedings of the National Academy of Sciences of the United States of America, v. 101, p. 12,952–12,956 https://doi.org/10.1073/pnas.0404472101.
Wang, X.D., Cawood, P.A., Zhao, H., Zhao, L.S., Grasby, S.E., Chen, Z.Q., and Zhang, L., 2019, Global mercury cycle during the end-Permian mass extinction and subsequent Early Triassic recovery: Earth and Planetary Science Letters, v. 513, p. 144–155, https://doi.org/10.1016/j.epsl.2019.02.026.
Wignall, P.B., 2015, The Worst of Times: How Life on Earth Survived Eighty Million Years of Extinction: Princeton, New Jersey, Princeton University Press, 224 p.

Printed in USA